SCIENTIFIC REP♀RTS

How two-dimensional bending can extraordinarily stiffen thin sheets

V. Pini*, J. J. Ruz*, P. M. Kosaka, O. Malvar, M. Calleja & J. Tamayo

Curved thin sheets are ubiquitously found in nature and manmade structures from macro- to nanoscale. Within the framework of classical thin plate theory, the stiffness of thin sheets is independent of its bending state for small deflections. This assumption, however, goes against intuition. Simple experiments with a cantilever sheet made of paper show that the cantilever stiffness largely increases with small amounts of transversal curvature. We here demonstrate by using simple geometric arguments that thin sheets subject to two-dimensional bending necessarily develop internal stresses. The coupling between the internal stresses and the bending moments can increase the stiffness of the plate by several times. We develop a theory that describes the stiffness of curved thin sheets with simple equations in terms of the longitudinal and transversal curvatures. The theory predicts experimental results with a macroscopic cantilever sheet as well as numerical simulations by the finite element method. The results shed new light on plant and insect wing biomechanics and provide an easy route to engineer micro- and nanomechanical structures based on thin materials with extraordinary stiffness tunability.

Small amounts of in-plane stress in thin elastic sheets give rise to a host of different and complex patterns[1–5]. Whereas the role of internal stress in the three dimensional configurations of thin sheets is starting to be understood, the reverse effect has received little attention. In fact, it is generally assumed that the deflection of thin sheets does not affect their stiffness within the framework of linear elasticity[6,7]. Under this prism, the stiffness of a thin sheet not subjected to stress is determined by its mechanical properties and its dimensions. We show here simple experiments with a cantilever made of a paper sheet that question this widely accepted assumption and reveal new fundamental properties of thin sheets. Our paper sheet is 297 mm long, 210 mm wide and 340 μm thick (Fig. 1). It is important to remark that the problem is scalable and the same phenomena can, for instance, be found in a microfabricated thin plate 297 μm long, 210 μm wide and 340 nm thick. The paper cantilever is obtained by fixing one of the ends of the sheet to a desk. The cantilever largely bends downwards due to gravity (Fig. 1a). If we add a small transversal curvature of 0.0035 mm^{-1} with positive sign (against gravity) to the clamped cantilever end, the sheet gets almost straight (Fig. 1b). This experiment reveals a first property: *the stiffness of cantilever sheets significantly increases with the transversal curvature*. We now rotate 180 degrees the transversally curved cantilever. The cantilever deflects downwards due to the gravity, more than before rotation, but substantially less than in the flat configuration (Fig. 1c). This experiment shows a second property referred to as *bending asymmetry: the upward and downward bending stiffness of a cantilever sheet is different when the cantilever is transversally curved*.

To understand why the paper cantilever stiffens when it is transversally curved, we make a second experiment with the paper sheet. We observe that whereas the sheet can be easily bent in one direction within the elastic regime (Fig. 2a,b), biaxial bending is not so straightforward (Fig. 2c). Far from achieving a parabolic-like surface[8], our sheet exhibits a characteristic wrinkle pattern that impedes biaxial bending. This experiment reveals a third property: *in-plane stresses are necessarily developed when the sheet is subject to biaxial bending*. We will show that this property is the origin of the stiffening of the paper cantilever when it is transversally bent. First, we mathematically demonstrate by appealing to simple geometry arguments this third property. We start with a thin sheet with length, width and thickness referred to as L, b and h, respectively, (Fig. 3). The structure is unrestrained at the edges and it is only subject to bending moments. The original flat structure must then transform into a structure with out-of-plane displacement $w_s(x, y)$ that obeys the following three topological constraints; the volume, contour length and contour width must remain constant. These constraints are consequence of that no in-plane stresses are applied to the sheet. For small displacements ($w_s(x, y) \ll L, b$), the constraints are mathematically

Institute of Microelectronics of Madrid (IMM-CSIC), Isaac Newton 8 (PTM), Tres Cantos, 28760 Madrid, Spain. *These authors contributed equally to this work. Correspondence and requests for materials should be addressed to J.T. (email: jtamayo@imm.cnm.csic.es)
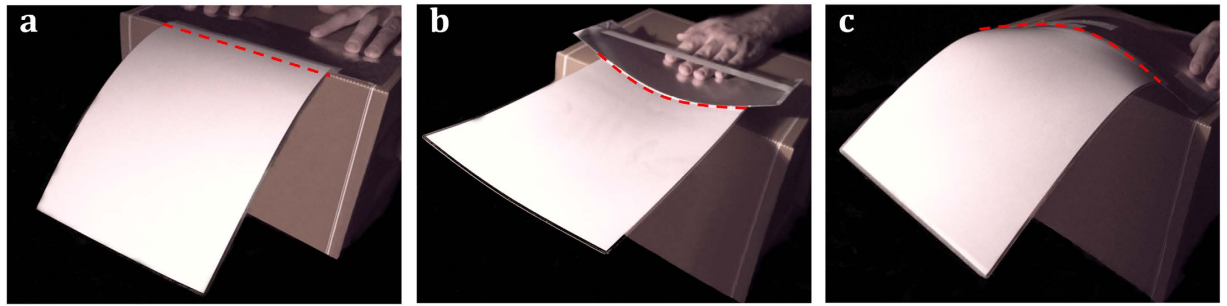
Figure 1. Stiffening of a paper sheet induced by transversal bending. (**a**) Photographs of a A4 paper cantilever sheet subject to gravity force when the transversal curvature is zero (**a**), positive (**b**) and negative (**c**).
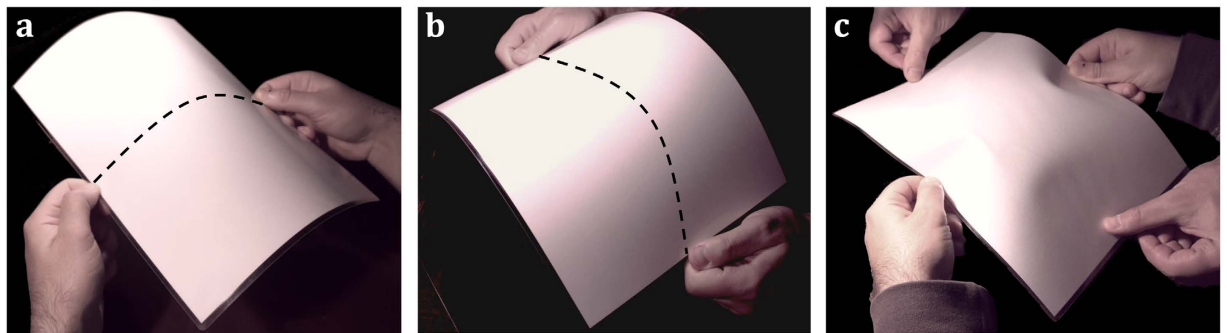

Figure 2. Wrinkling of a paper sheet subject to biaxial bending. Photographs of a A4 paper sheet manually subject to uniaxial bending in the transversal (**a**) and longitudinal (**b**) directions; and to biaxial bending (**c**).
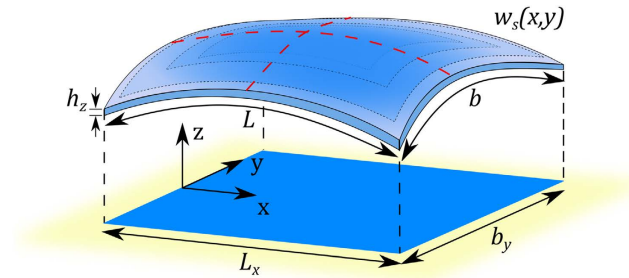

Figure 3. Schematic of the bending of an unrestrained thin sheet. The sheet in the flat state has length, width and thickness given by L, b and h respectively. Biaxial bending induces out-of-plane displacement (z direction) given by $w_s(x, y)$. The projections of the length and the width of the deformed sheet onto the x- and y- axes are given by L_x and b_y, respectively. The origin of the x-axis is at the left free edge of the undeformed plate, and the origins of the y- and z- axis are at the middle of the undeformed plate.

expressed by applying Pythagorean theorem to infinitesimal lengths in the chosen Cartesian coordinate system (Fig. 3),

$$bhL = \int_0^{L_x} \int_{-\frac{b_y}{2}}^{\frac{b_y}{2}} h_z \, dx dy \tag{1}$$

$$L = \int_0^{L_x} \left\{ 1 + \frac{1}{2} (\partial_x w_s)^2 \right\} dx \tag{2}$$

$$b = \int_{-\frac{b_y}{2}}^{\frac{b_y}{2}} \left\{ 1 + \frac{1}{2}(\partial_y w_s)^2 \right\} dy \tag{3}$$

where L_x and b_y are the projections of the length and the width of the deformed sheet onto the x- and y- axes, respectively; and h_z is the thickness along the z- axis given by,

$$h_z = h \left\{ 1 + \frac{1}{2}(\partial_x w_s)^2 + \frac{1}{2}(\partial_y w_s)^2 \right\} \tag{4}$$

Since there are more equations than unknowns, L_x and b_y, the system of equations, Eqns (1–3), is overdetermined and it is, in general, inconsistent. This is revealed by substituting Eqs (2), (3) and (4) into Eq. (1) which results in the paradoxical equation,

$$(L_x - L)(b_y - b) = 0 \tag{5}$$

Since $L_x \leq L$ and $b_y \leq b$, equation (5) can only be satisfied if the sheet is bent in one direction, as the length of the sheet in the orthogonal direction remains constant. Equation (5) is not satisfied in the case of biaxial bending, which implies that strains are necessarily generated, modifying the contour length of the sheet and thus violating Eqns (2) and (3).

Theory of the Stiffness of Curved Thin Sheets

In thin sheets, the energy cost of in-plane straining is very high, $\sim \frac{h}{L}$, in comparison with the bending energy $\sim \left(\frac{h}{L}\right)^3$. The most obvious manifestation of this effect is that small in-plane stresses in thin sheet give rise to formation of three dimensional configurations such as buckling or wrinkling-like instabilities[1,2,5]. We demonstrate the opposite phenomena; three dimensional configurations in thin sheets give rise to internal strain configurations. The curvature-induced in-plane strain significantly increases the elastic energy of the sheet, leading to large stiffening. The resolution of the strains that minimize the elastic energy cost in thin sheets poses a formidable theoretical challenge. We circumvent the enormous difficulty of the problem by starting with the thin sheet already deformed and calculating the energy cost associated to an additional small deformation. The initial deformation is referred to as static deformation and it may be plastic or/and elastic. The associated strains may also include geometric nonlinearities[9]. The second deformation is referred to as dynamic deformation and it must be elastic and sufficiently small to be described by linear strain-displacement relations. The out-of-plane displacements of the static and dynamic deformations are respectively given by $w_s(X, Y)$ and $\Delta w(X, Y)$, where $X = \frac{x}{L}$ and $Y = \frac{y}{b}$. Our proposed functions for the in-plane x and y displacements associated to the dynamic deformation are given by,

$$u(X, Y, z) = f(X, Y) - \partial_X \Delta w(X, Y)\left(\frac{z - w_s(X, Y)}{L}\right) \tag{6}$$

$$v(X, Y, z) = g(X, Y) - \partial_Y \Delta w(X, Y)\left(\frac{z - w_s(X, Y)}{\beta L}\right) \tag{7}$$

where $\beta \equiv \frac{b}{L}$. The first summand in Eqs (6) and (7) represent the in-plane displacement of the mid surface and the second summand the bending displacement. The proposed displacement field departs with respect to classical Kirchhoff-Love plate theory[7] in the following: i) the neutral plane is substituted by the curved surface, $w_s(X, Y)$ of the bent sheet and ii) the in-plane displacement of the mid surface is nonzero, albeit in-plane stresses are not exerted on the plate. The strain tensor induced by the dynamic deformation is given by,

$$\varepsilon = \begin{pmatrix} \dfrac{\partial_X u}{L} & \dfrac{1}{2}\left(\dfrac{\partial_Y u}{\beta L} + \dfrac{\partial_X v}{L}\right) & \dfrac{1}{2}\left(\partial_z u + \dfrac{\partial_X \Delta w}{L}\right) \\[2ex] \dfrac{1}{2}\left(\dfrac{\partial_Y u}{\beta L} + \dfrac{\partial_X v}{L}\right) & \dfrac{\partial_Y v}{\beta L} & \dfrac{1}{2}\left(\partial_z u + \dfrac{\partial_Y \Delta w}{\beta L}\right) \\[2ex] \dfrac{1}{2}\left(\partial_z u + \dfrac{\partial_X \Delta w}{L}\right) & \dfrac{1}{2}\left(\partial_z u + \dfrac{\partial_Y \Delta w}{\beta L}\right) & 0 \end{pmatrix} \tag{8}$$

We calculate the elastic energy of the system by using,

$$U = \frac{1}{2} L_x b_y C_{ijkl} \int_0^{\frac{L_x}{L}} dX \int_{-\frac{b_y}{2b}}^{\frac{b_y}{2b}} dY \int_{w_s(X,Y)-\frac{1}{2}h_z}^{w_s(X,Y)+\frac{1}{2}h_z} \varepsilon_{ij}\varepsilon_{kl} dz \tag{9}$$

where C_{ijkl} is the elastic tensor and Einstein summation convention is used. The unknown displacement functions, f and g, are obtained by solving the Euler-Lagrange equations corresponding to the elastic energy of the system. To find analytical solutions to the problem, the following assumptions must be adopted: i) the deformation of the

plate is symmetric about the y-axis of the thin plate and ii) the y-curvatures of the static and dynamic z displacements are independent of the y-coordinate. We refer the x- and y- directions to the longitudinal and transversal directions of the plate. For the sake of simplicity, we also assume that the plate is an isotropic material. The analytic solution of the problem is detailed in the Supplementary Materials (Sect. S1). We here provide the resulting potential energy that takes the form, $U = U_b + U_s$, where U_b is the bending energy and U_s is the in-plane straining energy. The bending energy is given by,

$$U_b = \frac{EL^5 \beta \eta^3}{24(1 - \nu^2)} \int_0^1 \{\Delta\kappa_y(X)^2 + 2\nu\Delta\kappa_y(X)\Delta\kappa_x(X) + \Delta\kappa_x(X)^2\} dX$$

(10)

where $\eta = \frac{h}{L}$, E is the Young modulus, and ν is the Poisson's ratio; $\Delta\kappa_x$ is the dynamic x- curvature at the longitudinal axis of the plate and $\Delta\kappa_y$ is the dynamic y- curvature. Importantly, the bending energy cost due to the dynamic deformation is independent of the previous static deformation of the plate.

The straining energy reads as,

$$U_s = \frac{EL^7 \beta^5 \eta}{1440} \int_0^1 (\kappa_x(X)\Delta\kappa_y(X) + \kappa_y(X)\Delta\kappa_x(X))^2 dX$$

(11)

where $\kappa_x(X)$ is the static x-curvature at the longitudinal axis of the plate and $\kappa_y(X)$ is the static y- curvature. Interestingly, the straining energy depends on the orthogonal coupling between the static and dynamic curvatures. The straining energy is zero when the sheet is only bent in one direction (e.g. $\Delta\kappa_y = \kappa_y = 0$). This is in consistency with the topological constraints described above; uniaxial bending is compatible with zero straining of the neutral surface. However, in-plane stresses necessarily come up when the sheet, for instance, is initially bent in the transversal direction and then it is longitudinally bent. The in-plane stresses that act as a pulling force against the longitudinal bending.

We analyze the practical case, in which i) the initial static curvatures are constants and ii) the curved sheet is subject to longitudinal bending moment, so $\Delta\kappa_y(X) \approx -\nu\Delta\kappa_x(X)$. The relative change of stiffness in this case is independent on how the load is distributed along the plate in the dynamic deformation step,

$$\frac{\Delta k}{k} = \frac{U_s}{U_b} = \frac{L^2}{60} \frac{\beta^4}{\eta^2} (\kappa_y - \nu\kappa_x)^2$$

(12)

Equation (12) was compared with numerical results by the finite element method (FEM), showing an error below 10% for free plates with $\beta < 0.4$ (Supplementary Sect. S2). A glance at equation (12) allows direct understanding of the basic mechanisms of plate stiffening due to curvature. The increase of the stiffness scales like $\sim\frac{\beta^4}{\eta^2}$. Thus, in the limit of very thin plates $\eta \ll 1$, the stiffness may be dominated by the initial curvatures of the plate. The quartic dependence on β indicates that this is a purely plate effect; the stiffening goes to zero in the limit of narrow beams ($\beta \ll 1$). The effect of longitudinal curvature goes as $\sim\nu^2$, being significantly smaller than the effect of transversal curvature. Transversal curving seems to be the most economical way to stiffen a thin plate structure. This may be the case of plant leaves. It is well-known the leaf-shapes have been optimized during evolution to absorb sufficient light and facilitate gas exchange[10]. From this point of view, leaves must be as wide, flat and thin as possible. However, leaf shape must also be optimized from the mechanical point of view; the leaf must support its own weight and external dynamic forces such as the pressure of winds[11]. Leaf curvature is genetically controlled and it can be modified at wish in some species by gene mutation[12]. The large influence of curvature on the stiffness of thin and wide sheets suggests that leaf curvature has been targeted by evolution for optimization of their biological and structural functions. The effect of bending asymmetry observed with the paper sheet (Fig. 1) can be explained by the coupling term in Eq. (12), $\sim-\nu\kappa_x\kappa_y$. The bending stiffness of a thin plate with x- and- y- curvatures of opposite sign is higher than in the case of x- and y- curvatures with the same sign. Bending asymmetry plays a key role in the flight of insects. Detailed FEM simulations of insect wings have shown that chordwise camber of the insect wings induces significant wing stiffening and the coupling between chordwise and spanwise camber is the origin of the dorsal-ventral bending asymmetry[13]. Here, we provide simple analytical equations that enable an intuitive understanding of this phenomenon.

Equation (12) was deduced for plates with free edges. However, it is common in nature and engineering to find these structures with one of the edges clamped. In these cases, the transversal curvature is zero at the clamping end and it exponentially increases in the x direction with a characteristic length given by the cantilever's width, tending to reach the asymptotic value (κ_y)[14]. We accordingly modify equation (12) to include the clamping effect,

$$\frac{\Delta k}{k} = \frac{L^2}{60} \frac{\beta^4}{\eta^2} e^{-c\beta} (\kappa_y - \nu\kappa_x)^2$$

(13)

The constant c depends on the shape of the dynamic deformation and must be computed by fitting Eq. (13) to FEM simulations. For the case of flexural bending in the fundamental vibration mode, $c \approx 3.095$. The error of Eq. (13) is below 5% when compared with FEM simulations for $\beta < 0.4$ (Supplementary Sect. S3).

Comparison of the Theory with a Experiment Based on a Macroscopic Cantilever Plate

We performed an easy experiment with a homebuilt macroscopic aluminum cantilever plate to validate our theoretical predictions (Fig. 4a). A step force was manually applied to the cantilever free end and the transient vibration was recorded by a smartphone camera (Fig. 4b) (Suppl. Sect. S4). The resonant frequency of a plate is related
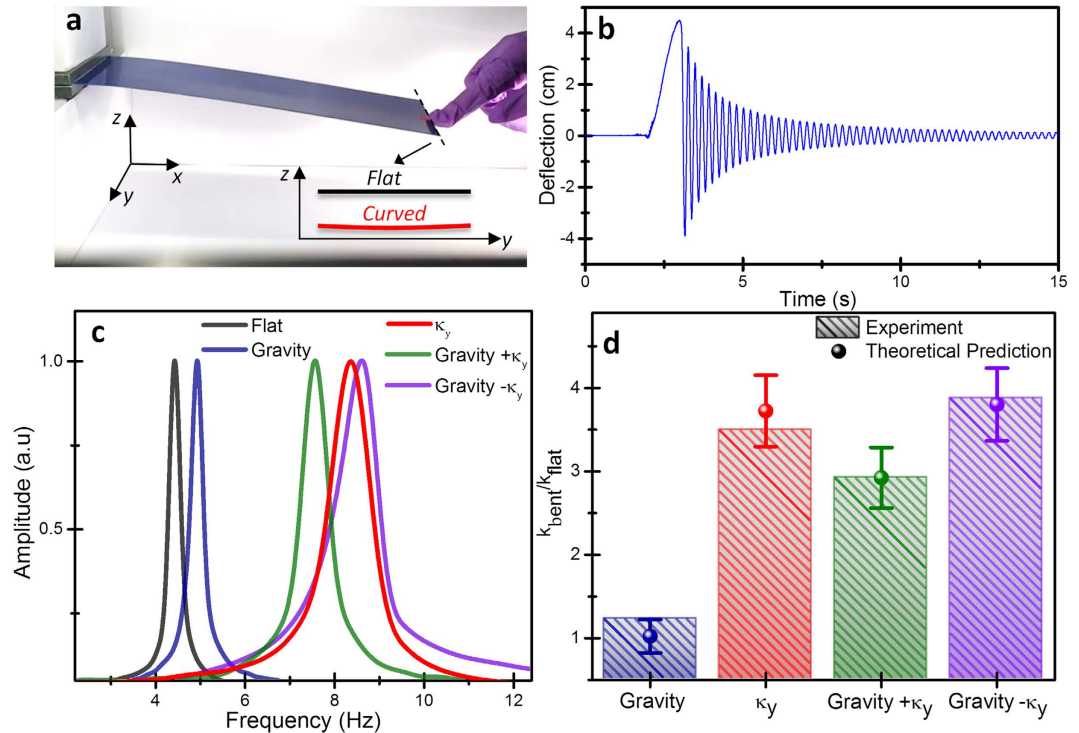
Figure 4. Experiment with a home-made cantilever plate. (**a**) Photograph of the macroscopic cantilever plate. The dimensions of the cantilever are $29 \times 10 \times 0.0645\,cm^3$. The cantilever was set into oscillation by applying a step force at the free end by one of our fingers. The inset shows the scaled profile of the free end of the cantilever in yz plane in the flat and curved configurations. (**b**) Transient oscillation of the microcantilever plate. (**c**) Frequency response of the cantilever at the different curvature configurations. **Flat** denotes the flat cantilever vertically oriented with respect to gravity; **Gravity** label the flat cantilever in horizontal position; κ_y denotes the cantilever with transversal curvature (inset of **a**) at the vertical position; **Gravity** $+ \kappa_y$ and **Gravity** $- \kappa_y$ denotes the transversally bent cantilever at the horizontal position with curvature inward and outward gravity, respectively. (**d**) Comparison between theory and experiment of the ratio between the stiffness of the bent cantilever and the flat cantilever at vertical position.

to the spring constant, k, by the harmonic oscillator equation $\omega_o = \sqrt{k/m}$ where m is the mass of the plate. Figure 4c summarizes the values of the resonance frequency for different curvature configurations. The flat cantilever plate at vertical orientation shows the lowest resonance frequency of about $4.4\,Hz$. When the cantilever is horizontally oriented, gravity induces longitudinal bending and the resonance frequency slightly increases to $4.9\,Hz$. The aluminum sheet was then transversally bent with very small curvature ($\kappa_y = 1.15\,m^{-1}$, see inset in Fig. 4a) and then clamped. At the vertical orientation, the resonance frequency of the transversally curved cantilever largely increased to $8.4\,Hz$ that is equivalent to an increase of the stiffness of 3.6 times. This proves the fundamental role of the transversal curvature in the stiffness of thin plates. To observe the bending asymmetry effect, the transversally curved cantilever was horizontally oriented with the transversal curvature inwards and outwards gravity. In consistency with our theory, in the first case, the resonance frequency decreases $0.7\,Hz$, with respect to the transversally bent cantilever at the vertical position, whereas, in the second case the resonance frequency increases $0.3\,Hz$. In order to quantitatively compare these results with the theory, we must extend our theoretical model to the case in which the static curvatures are not uniform as it is the case of gravity-induced bending (Suppl. Sect. S4). The comparison between theory and experiment shows a very good agreement (Fig. 4d).

Conclusions

Here, we demonstrate that small amounts of two-dimensional bending of thin plates lead to the development of in-plane stresses, and thus bending is not in general so energetically cheap as believed hitherto. Biaxial curving of thin sheets is perhaps the most efficient way to reinforce the mechanical stability of thin sheets. This ancient mechanism found in nature and in man-made structures has remained unexplained in physics. The theoretical model and simple equations provided here solve this long-standing problem shedding light in our understanding of thin sheet mechanics and bringing new and useful mathematical tools to a wide variety of fields such as natural science[15], mechanical engineering and micro/nanotechnology[16–20].

References

1. Marder, M., Deegan, R. D. & Sharon, E. Crumpling, buckling, and cracking: elasticity of thin sheets. *Phys. Today* **60,** 33 (2007).
2. Li, B., Cao, Y.-P., Feng, X.-Q. & Gao, H. Mechanics of morphological instabilities and surface wrinkling in soft materials: a review. *Soft Matter* **8,** 5728–5745 (2012).

3. Starostin, E. L. & Van Der Heijden, G. H. M. The shape of a Möbius strip. *Nat. Mater.* **6,** 563–567 (2007).
4. Vliegenthart, G. A. & Gompper, G. Forced crumpling of self-avoiding elastic sheets. *Nat. Mater.* **5,** 216–221 (2006).
5. Kim, P., Abkarian, M. & Stone, H. A. Hierarchical folding of elastic membranes under biaxial compressive stress. *Nat. Mater.* **10,** 952–957 (2011).
6. Lachut, M. J. & Sader, J. E. Effect of surface stress on the stiffness of thin elastic plates and beams. *Phys. Rev. B* **85,** 085440 (2012).
7. Landau, L. D. & Lifshitz, E. Theory of Elasticity. *Course of Theoretical Physics* **3,** 109 (1986).
8. Sader, J. E. Surface stress induced deflections of cantilever plates with applications to the atomic force microscope: rectangular plates. *J. Appl. Phys.* **89,** 2911–2921 (2001).
9. Villanueva, L. G. *et al.* Nonlinearity in nanomechanical cantilevers. *Phys. Rev. B* **87,** 024304 (2013).
10. Moulia, B. Leaves as shell structures: double curvature, auto-stresses, and minimal mechanical energy constraints on leaf rolling in grasses. *J. Plant Growth Regul.* **19,** 19–30 (2000).
11. Niklas, K. J. A mechanical perspective on foliage leaf form and function. *New Phytol.* **143,** 19–31 (1999).
12. Rolland-Lagan, A.-G., Remmler, L. & Girard-Bock, C. Quantifying shape changes and tissue deformation in leaf development. *Plant Physiol.* **165,** 496–505 (2014).
13. San Ha, N., Truong, Q. T., Goo, N. S. & Park, H. C. Biomechanical Properties of Insect Wings: The Stress Stiffening Effects on the Asymmetric Bending of the Allomyrina dichotoma Beetle's Hind Wing. *PLoS ONE* **8** (2013).
14. Tamayo, J., Ruz, J. J., Pini, V., Kosaka, P. & Calleja, M. Quantification of the surface stress in microcantilever biosensors: revisiting Stoney's equation. *Nanotechnology* **23,** 475702 (2012).
15. Park, Y. *et al.* Metabolic remodeling of the human red blood cell membrane. *Proc. Natl. Acad. Sci. USA* **107,** 1289–1294 (2010).
16. Tamayo, J., Kosaka, P. M., Ruz, J. J., San Paulo, Á. & Calleja, M. Biosensors based on nanomechanical systems. *Chem. Soc. Rev.* **42,** 1287–1311 (2013).
17. Boisen, A., Dohn, S., Keller, S. S., Schmid, S. & Tenje, M. Cantilever-like micromechanical sensors. *Rep. Prog. Phys.* **74,** 036101 (2011).
18. Karabalin, R. B., Villanueva, L. G., Matheny, M. H., Sader, J. E. & Roukes, M. L. Stress-induced variations in the stiffness of micro- and nanocantilever beams. *Phys. Rev. Lett.* **108,** 236101 (2012).
19. Pini, V. *et al.* Shedding light on axial stress effect on resonance frequencies of nanocantilevers. *ACS Nano* **5,** 4269–4275 (2011).
20. Ruz, J. J., Tamayo, J., Pini, V., Kosaka, P. M. & Calleja, M. Physics of nanomechanical spectrometry of viruses. *Sci. Rep.* **4,** 6051 (2014).

Acknowledgements

Author Contributions

V.P., J.J.R., M.C. and J.T. conceived and designed the work. V.P., J.J.R. and J.T. developed the theoretical model. V.P. and J.J.R. carried out the FEM simulations. O.M., V.P., J.J.R. and P.K. carried out the experiments. J.T. wrote the manuscript with inputs from all authors. All the authors analysed the data, discussed the results and commented on the manuscript.

Additional Information

Supplementary information accompanies this paper at http://www.nature.com/srep

Competing financial interests: The authors declare no competing financial interests.

How to cite this article: Pini, V. *et al.* How two-dimensional bending can extraordinarily stiffen thin sheets. *Sci. Rep.* **6**, 29627; doi: 10.1038/srep29627 (2016).